

Vapor-liquid Interface of Argon by Using a Test-area Simulation Method

Song Hi Lee

Department of Chemistry, Kyungsoong University, Busan 608-736, South Korea. *E-mail: shlee@ks.ac.kr
Received October 17, 2011, Accepted November 17, 2011

A test-area molecular dynamics simulation method for the vapor-liquid interface of argon through a Lennard-Jones intermolecular potential is presented in this paper as a primary study of interfacial systems. We found that the calculated density profile along the z-direction normal to the interface is not changed with time after equilibration and that the values of surface tension computed from this test-area method are fully consistent with the experimental data. We compared the thermodynamic properties of vapor argon, liquid argon, and argon in the vapor-liquid interface. Comparisons are made with kinetic and potential energies, diffusion coefficient, and viscosity.

Key Words : Vapor-liquid interface, Test-area method, Surface tension, Molecular dynamics simulation

Introduction

Interfacial systems are of considerable interest to both nature and practical technologies. An understanding of interfaces and inhomogeneous systems is essential to all areas of industrial processes. For example, the surface tension between a liquid and its vapor or two coexisting liquids is of central importance in understanding capillary rise and the solubilization of immiscible fluids.

It is therefore natural that molecular theories of inhomogeneous systems are now well developed,¹⁻³ with major advance since the pioneering work of van der Waals.⁴ Molecular dynamics simulation techniques are also routinely used to examine inhomogeneous systems. It is relatively straight forward to simulate the interfacial profile between two coexisting fluid¹ or a fluid in contact with a solid surface,⁵ and complex systems including surfactant solutions,⁶ biological membranes,^{7,8} and nematic liquid-crystalline films,⁹⁻¹³ and coexisting liquid-crystalline films phases which possess orientational and translational order¹⁴ have now been simulated.

There are three general types of simulation techniques to determine the surface tension γ of fluids. The first, and most widespread, class of technique involves a mechanical routine which requires the calculation of the tensional components of the pressure.¹ In the case of a planar interface perpendicular to the z axis, the surface tension is given by,

$$\gamma = \int_{-\infty}^{\infty} dz [p_N(z) - p_T(z)] = L_z [\bar{p}_N - \bar{p}_T], \quad (1)$$

where $p_N(z)$ are $p_T(z)$ the normal and tangential component of the pressure tensor at position z, respectively. \bar{p}_N and \bar{p}_T are the macroscopic components of the pressure tensor defined in terms of the volume average of their local components counterparts¹⁵; $p_N(z) = p_{zz}(z)$ and $p_T(z) = p_{xx}(z) = p_{yy}(z) = [p_{xx}(z) + p_{yy}(z)]/2$. The pressure tensor is given by

$$p_{\alpha\beta} = \frac{1}{V} \sum_i p_{i\alpha\beta} = \frac{1}{V} \sum_i [m v_{i\alpha} \cdot v_{i\beta} + \sum_{j \neq i} r_{ij\alpha} \cdot f_{ij\beta}] \quad (2)$$

with $\alpha\beta = xx, yy, \text{ and } zz$. Considering two vapor-liquid interfaces in this test-area simulation method, γ turns out to be

$$\gamma = \frac{L_z}{2} [\bar{p}_N - \bar{p}_T]. \quad (3)$$

The second route to the surface tension involves a thermodynamic perspective in which the free-energy difference between two system with different interfacial area is determined to estimate the surface tension (the method of Bennet¹⁶). The third class of technique is based on the concepts of finite-size scaling. In the case of the method developed by Binder¹⁷ one estimates a Landau free-energy barrier between coexisting phases from a simulation of the density of the states, which in the limit of large system sizes can be related to the surface tension.

In this study we present a test-area molecular dynamics simulation method to determine the surface tension of liquid argon as a first primary study for interfacial systems. This approach will be applied to more complicated molecules such as water in our future studies. The secondary purpose of this study is to compare the thermodynamic properties of vapor argon, liquid argon, and argon in the vapor-liquid interface. Comparisons are made with kinetic and potential energies, diffusion coefficient, and viscosity.

Test-area Simulation Method

Two states of liquid argon are chosen as shown Table 1. The usual Lennard-Jones (LJ) 12-6 potential for the interaction between argon molecules is used with LJ parameters, $\sigma = 0.34$ nm and $\epsilon/k_B = 120$ K, where k_B is the Boltzmann constant. The inter-atomic potential is truncated at $r_c = 4\sigma$ and long-range corrections are applied to the energy, pressure, etc. due to the potential truncation.¹⁸ The time integrations for the equation of translational motion is solved using the velocity-Verlet algorithm¹⁹ with a time step of 5×10^{-15} second (5 fs). The temperature is kept constant by

Table 1. Two chosen states of liquid argon. L is the length of initial cubic simulation box. E_K , E_P , and E_T are the kinetic, potential, and total energies, and D and η are the diffusion coefficient and viscosity obtained from MD simulation. Uncertainties (standard deviation) in the last reported digit(s) are given in the parenthesis. Some results are compared with the experimental data²³

| T (K) | ρ (g/cm ³) | L (nm) | E_K (kJ/mol) | $-E_P$ (kJ/mol) | $-E_T$ (kJ/mol) (exp.) | D (10 ⁻⁵ cm ² /sec) | η (mP) |
|-------|-----------------------------|----------|----------------|-----------------|------------------------|---|-------------|
| 94.4 | 1.374 | 4.8753 | 1.177 | 5.703 | 4.526 (4.3804) | 2.489(47) | 2.519(40) |
| 119.8 | 1.176 | 5.1348 | 1.494 | 4.767 | 3.273 (3.1819) | 6.067(65) | 1.227(7) |

using a Nose-Hoover^{20,21} thermostat. These systems of $N = 2400$ molecules of argon are fully equilibrated in cubic boxes with the usual periodic boundary condition. The kinetic and potential energies, diffusion coefficient (Eq. (4)), and viscosity (Eq. (5)) of the two states of liquid argon are computed and listed in Table 1.

In order to simulate the liquid-vapor interface by using the test-area method, the above equilibrated systems of liquid argon are placed in between two empty regions. The initial condition is a liquid cubic in the middle of the z direction in the simulation domain and the vapor sides are set as a vacuum (see Fig. 1(a)). Molecular dynamics (MD) simulations are carried out at constant T and volume V in a

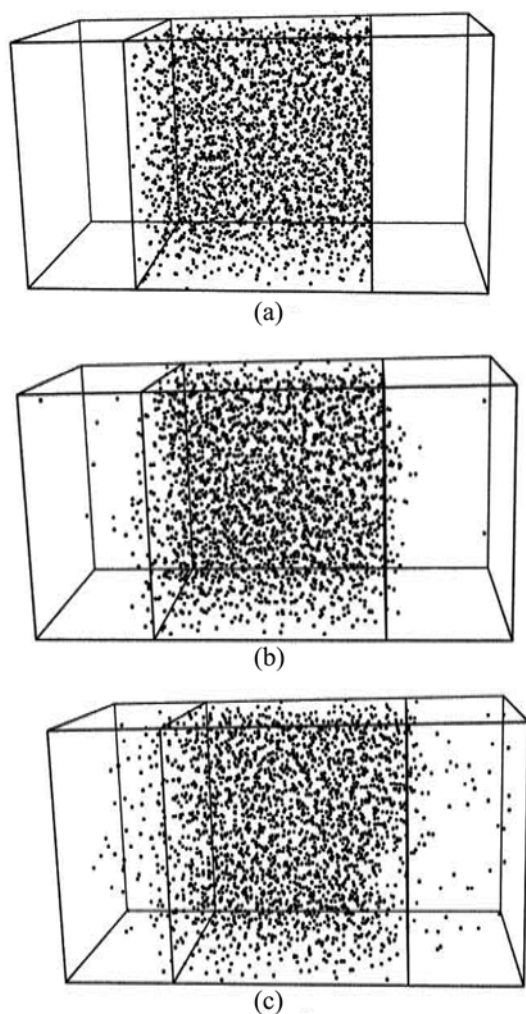


Figure 1. Snapshots of argon molecules (a) in the initial cubic simulation box, and (b) after equilibration at 94.4 K, and (c) at 119.8 K.

rectangular box of dimensions $L_x = L_y \approx 4.8$ -5.2 nm according to the system density at a given temperature (see Table 1), and $L_z = 10$ nm with the usual periodic boundary condition of the x -, y -, and z -directions. Figure 1(b) and (c) are snapshots of the equilibrium states of the simulation systems at 94.4 K and 119.8 K, respectively. The equilibrium properties are averaged over 5 blocks of 200,000 time steps after equilibration for 500,000 time steps and the configuration of all the argon molecules is stored every 4 time steps for further analyses. The calculated density profile of each block along the z -direction normal to the interface is not changed with time after equilibration (see Fig. 2).

The diffusion coefficient of particle i is obtained through the Einstein formula from mean square displacements:

$$D_i = \frac{1}{6} \lim_{t \rightarrow \infty} \frac{d \langle [r_i(t) - r_i(0)]^2 \rangle}{dt} \quad (4)$$

The viscosity contributed by particle i is given by

$$\eta_i = \frac{V}{k_B T} \int_0^\infty dt \langle p_{i\alpha\beta}(t) \cdot p_{i\alpha\beta}(0) \rangle \quad (5)$$

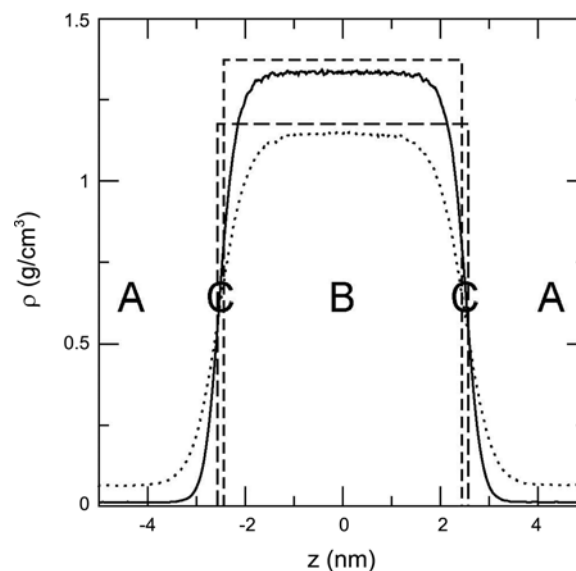


Figure 2. Vapor-liquid density profile, $\rho(z)$ in unit of g/cm³, along the z -direction normal to the interface obtained from MD simulation for two chosen states of liquid argon (solid line: 94.4 K and dotted line: 119.8 K). The dashed and long-dashed lines represent the density profiles in the initial cubic of liquid argon at 94.4 K and 119.8 K, respectively. Region A: vapor argon ($|z| > 3.5$ nm for 94.4 K and $|z| > 4$ nm for 119.8 K), B: liquid argon ($|z| < 1.5$ nm for 94.4 K, and $|z| < 1$ nm for 119.8 K), and C: argon in the vapor-liquid interface ($1.5 < |z| < 3.5$ nm for 94.4 K, and $1 < |z| < 4$ nm for 119.8 K).

where $p_{i\alpha\beta}$ is given in Eq. (2) with $\alpha\beta = xy, xz,$ and yz since $p_{i\alpha\beta} = p_{i\beta\alpha}$ for LJ system. The viscosity in a given region, R, is equal to $\eta_R = \sum_{i \in R} \eta_i$.²²

Results and Discussion

The volume of a vapor side at 94.4 K shown in Figure 1 is equal to $(4.8753 \text{ nm})^2 \times (10 \text{ nm} - 4.8753 \text{ nm}) = 60.9 \text{ nm}^3$. How many air molecules in this volume at 94.4 K? At room temperature (298.15 K) the density of air is equal to 1.1839 kg/m³ which correspond to the number density of 0.0246 nm⁻³. There exist 1.5 air molecules in the vapor side at 298.15 K. Assuming 5 air molecules at 94.4 K, the assumption for the vapor sides as a vacuum is verified when compared with 2400 Argon molecules in the volume of $(4.8753 \text{ nm})^3 = 115.9 \text{ nm}^3$.

The values of the surface tension [Eq. (3)] as obtained from MD simulation are reported in Table 2 for the two states of liquid argon. The vapor and liquid densities (ρ_v and ρ_l) at coexistence, the average portion (N(%)) of argon molecules in each phase, the thickness (t) of the vapor-liquid interface, and the macroscopic values of the normal and tangential components (\bar{p}_N and \bar{p}_T) of the pressure tensor are also included in this table. For a planar interface, \bar{p}_N does not depend on z. The calculated value of \bar{p}_N is constant throughout the system and equal to the equilibrium pressure, p. The values of \bar{p}_N for T = 94.4 and 119.8 K are in good agreement with the experimental data.²³ Comparison of surface tensions for both temperatures with the experimental data²³ is also in excellent agreement. The previous test-area Monte-Carlo simulation study¹⁵ reported $\gamma = 9.80 \text{ mN/m}$ at 90 K and 8.54 mN/m at 96 K, and $\gamma = 3.51 \text{ mN/m}$ at 120 K for a LJ system with $r_c = 2.5\sigma$ which are too low compared

to the experimental data.²³ With $r_c = 5.5\sigma$, $\gamma = 13.86 \text{ mN/m}$ at 90 K and 12.47 mN/m at 96 K, and $\gamma = 6.53 \text{ mN/m}$ at 120 K which are too high compared to the experimental data.²³ Most recently, a weighted density functional theory and MD simulation²⁴ study for liquid argon systems with two-body and three-body interactions²⁵ predicted much better agreement of surface tension with the experimental data²³ than with only two-body interactions.²⁶

In Figure 2 we present the density profile, $\rho(z)$ in unit of g/cm³, along the z-direction normal to the interface obtained from MD simulation for argon at the two states of liquid argon. The profile is averaged over 5 blocks of 200,000 time steps and 5 block-averaged profiles are completely indistinguishable each other. This indicates that vaporization and condensation occur simultaneously and at equal rates-dynamic equilibrium. The fact that the profile is essentially symmetric about the midpoint $z = 0$ (see Fig. 2) provides additional evidence that the inhomogeneous system is properly equilibrated. Figure 1(b) and (c) show roughly how many argon molecules are in the vapor at 94.4 K and 119.8 K, respectively. Regions of vapor argon, liquid argon, and argon in the vapor-liquid interface are defined as A, B, and C as described in Figure 2. The thicknesses of the vapor-liquid interface are equal to the lengths of region C in Figure 2 which are found to be 2.0 and 3.0 nm for T = 94.4 and 119.8 K as shown in Table 2.

The vapor and liquid densities at coexistence, ρ_v and ρ_l , are obtained from the running average of the corresponding density profile and are in good agreement with the experimental data.²³ The liquid densities (ρ_v) are reduced by 3.0 and 2.7% from the bulk densities (ρ) and the average densities (ρ_{v-l}) of argon in the vapor-liquid interface are nearly halves of the liquid densities (ρ_l) for T = 94.4 K and 119.8 K.

Table 2. Values of the surface tension (γ) obtained from MD simulation. ρ_v and ρ_l are the vapor and liquid densities at coexistence, ρ_{v-l} is the average density of argon in the vapor-liquid interface, N (%) is the average portion of argon molecules in each phase, t is the thickness of the vapor-liquid interface, and \bar{p}_N and \bar{p}_T are the macroscopic values of the normal and tangential components of the pressure tensor. Uncertainties (standard deviation) in the last reported digit(s) are given in the parenthesis. Some results are compared with the experimental data²³

| T (K) | ρ_v (g/cm ³), N_v (%) (exp.) | ρ_l (g/cm ³), N_l (%) (exp.) | ρ_{v-l} (g/cm ³) | t (nm) | \bar{p}_N (bar) (exp.) | \bar{p}_T (bar) | γ (mN/m) (exp.) |
|-------|--|--|--------------------------------------|-----------|-----------------------------|-------------------|---------------------------|
| 94.4 | 0.0122(5), 0.537 (0.01089) | 1.333(4), 59.7 (1.3507) | 0.6655 | 2.0 | 2.22(12) (2.0198) | -19.53(36) | 10.88(20) (10.767) |
| 119.8 | 0.0649(15), 2.05 (0.05947) | 1.145(4), 38.0 (1.1645) | 0.6030 | 3.0 | 13.10(31) (11.997) | 2.68(82) | 5.21(28) (5.000) |

Table 3. Comparison of thermodynamic properties for vapor argon (A), liquid argon (B), and argon in the vapor-liquid interface (C) at the two states of liquid argon. Some results are compared with the experimental data²³

| T(K) | E_K (kJ/mol) | | | $-E_P$ (kJ/mol) | | | D ($10^{-5} \text{ cm}^2/\text{sec}$) | | | η (mP) | | |
|-------|----------------|-------|-------|-----------------|-------|-------|---|-------|-------|--------------------|-------------------|-------|
| | A | B | C | A | B | C | A | B | C | A (exp.) | B (exp.) | C |
| 94.4 | 1.248 | 1.176 | 1.179 | 0.083 | 5.541 | 5.088 | 110.7 | 2.823 | 6.335 | 0.0585 (0.0780) | 2.149 (2.1612) | 0.606 |
| 119.8 | 1.513 | 1.492 | 1.495 | 0.341 | 4.654 | 3.743 | 92.22 | 5.831 | 12.25 | 0.0875 (0.1060) | 1.156 (1.0946) | 0.471 |

The Gibbs dividing surfaces (GDS) are estimated as at 2.52 and 2.58 nm for $T = 94.4$ and 119.8 K. The values of GDS are almost coincided to halves of lengths of initial cubic simulation boxes (2.44 and 2.57 nm) as seen in Figure 2. The average portion, $N(\%)$, of argon molecules in each phase is related to the thickness of each phase. The thicknesses of liquid argon for $T = 94.4$ and 119.8 K are estimated as 3.0 and 2.0 nm, respectively. Ignoring numbers of vapor argon molecules and considering half numbers of argon molecules in the vapor-liquid interface, $N_B(\%)$ [= $N_I(\%)$] and $N_C(\%)$ are almost 60 and 40 for $T = 94.4$ K and *vice versa* for $T = 119.8$ K.

We have computed a number of thermodynamics properties of each phase and listed in Tables 1 and 3. First, the calculated total energies of the two systems are within 3.2 and 2.8%, respectively, compared with the experimental internal energies²³ as shown in Table 1. While the kinetic energies of liquid argon and argon in the vapor-liquid interface are almost the same as that of bulk argon for both temperatures, E_K of vapor argon is slightly increased as expected from the change of density. On the other hand, the potential energies of all the phases for both temperatures are decreased due to the low densities. E_P of liquid argon is slightly decreased but that of vapor argon is much less than that of bulk argon due to the negligible density of vapor argon.

Dramatic change in diffusion coefficient of vapor argon represents the gas state of argon. The typical diffusion coefficient of argon gas at 1 bar and 298.15 K is about 10^{-1} cm²/sec. D of liquid argon is slightly increased at $T = 94.4$ K and decreased at $T = 119.8$ K when compared with that of bulk argon. D of argon in the vapor-liquid interface is more than twice that of bulk argon which indicates the argon molecules are not in the gas state. Finally, the calculated viscosities of vapor argon and liquid argon are in good agreement with the experimental data.²³ η of liquid argon is slightly decreased and that of vapor argon is much decreased as in the gas state when compared with that of bulk argon. The typical viscosity of argon gas at 1 bar and 298.15 K is about 0.2 mP. η of argon in the vapor-liquid interface is less than one-third that of bulk argon, which also indicates the argon molecules are not in the gas state.

Conclusion

We have carried out molecular dynamics (MD) simulations of vapor-liquid interface of argon at $T = 94.4$ K and 119.8 K using a test-area simulation method to calculate the surface tension of liquid argon. Five different block-averaged density profiles along the z-direction normal to the interface are completely indistinguishable each other. The cal-

culated values of the surface tension, the vapor and liquid densities at coexistence, the macroscopic normal component of the pressure tensor, the viscosity of vapor argon and liquid argon obtained from MD simulations are in good agreement with the experimental data²³ for both temperatures. The kinetic and potential energies, diffusion coefficients, and viscosities of vapor argon, liquid argon, and argon in the vapor-liquid interface for both temperatures are compared and represent the state of each phase properly.

Acknowledgments. This research was supported by Kyungshung University Research Grants in 2011.

References

- Rowlinson, J. S.; Widom, B. *Theory of Capillarity*; Oxford: Clarendon: 1982.
- Henderson, D. *Fundamentals of Inhomogeneous Fluids*; New York: Dekker: 1992.
- Davis, H. T. *Statistical Mechanics of Phases, Interfaces, and Thin Films*; Weinheim: VCH: 1996.
- (a) van der Waals, J. D. *Z. Phys. Chem.* **1894**, *13*, 657. (b) English translation, Rowlinson, J. S. *J. Stat. Phys.* **1979**, *20*, 197.
- Nicholson, D.; Parsonage, N. G. *Computer Simulation and Statistical Mechanics of Adsorption*; London: Academic: 1982.
- Shelley, J. C.; Shelly, M. Y. *Curr. Opin. Colloid Interface Sci.* **2000**, *5*, 101.
- Tobias, D. J.; Tu, K. C.; Klein, M. L. *Curr. Opin. Colloid Interface Sci.* **1997**, *2*, 15.
- Saiz, L.; Klein, M. L. *Acc. Chem. Res.* **2002**, *35*, 482.
- Martín del Río, E.; de Miguel, E. *Phys. Rev. E* **1997**, *55*, 2916.
- Bates, M.; Zannoni, C. *Chem. Phys. Lett.* **1997**, *280*, 40.
- Mills, S. J.; Care, C. M.; Near, M. P.; Cleaver, D. J. *Phys. Rev. E* **1998**, *58*, 3284.
- de Miguel, E.; Martín del Río, E. *Int. J. Mod. Phys. C.* **1999**, *10*, 431.
- Akino, N.; Schmid, F.; Allen, M. P. *Phys. Rev. E* **2001**, *63*, 041706.
- Galindo, A.; Haslam, A. J.; Varga, S.; Jackson, G.; Vanakaras, A.; Photinos, D. J.; Dunmur, D. A. *J. Chem. Phys.* **2004**, *121*, 12740.
- Gloor, G. J.; Jackson, G.; Blas, F. J.; de Miguel, E. *J. Chem. Phys.* **2005**, *123*, 134703.
- Bennet, C. H. *J. Comput. Phys.* **1976**, *22*, 245.
- Binder, K. *Phys. Rev. A* **1982**, *25*, 1699.
- Allen, M. P.; Tildesley, D. J. *Computer Simulation of Liquids*; Oxford: Oxford Univ. Press: 1987; p 64.
- Swope, W. C.; Andersen, H. C.; Berens, P. H.; Wilson, K. R. *J. Chem. Phys.* **1982**, *76*, 637.
- Hoover, W. G. *Phys. Rev. A* **1985**, *31*, 1695.
- Nosé, S. *Mol. Phys.* **1984**, *52*, 255.
- Lee, S. H. *Bull. Kor. Chem. Soc.* **2007**, *28*, 1371.
- NIST Chemistry WebBook. <http://webbook.nist.gov/chemistry/fluid> (accessed 2011).
- Zhou, D.; Zeng, M.; Mi, J.; Zhong, C. *J. Phys. Chem. B* **2011**, *115*, 57.
- Lee, J. K.; Barker, J. K. *J. Chem. Phys.* **1974**, *60*, 1976.
- Janecek, J. *J. Phys. Chem. B* **2006**, *110*, 6264.